IEEE Photonics Journal
An IEEE Photonics Society Publication

Open Access

AC Stark Effect on Vortex Spectra Generated by Circularly Polarized Pulses

Volume 11, Number 3, June 2019

Meng Li
Guizhong Zhang
Xin Ding
Jianquan Yao

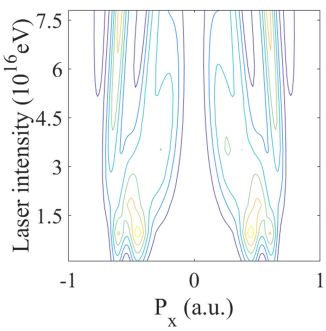

DOI: 10.1109/JPHOT.2019.2916106
1943-0655

AC Stark Effect on Vortex Spectra Generated by Circularly Polarized Pulses

Meng Li,[1,2] **Guizhong Zhang**,[1] **Xin Ding**,[1] **and Jianquan Yao**[1]

[1]Key Lab of Optoelectronic, College of Precision Instrument and Optoelectronics Engineering, Tianjin University, Tianjin 300072, China
[2]Key Laboratory of Operation Programming & Safety Technology of Air Traffic Management. Civil Aviation University of China, Tianjin 300300, China

DOI:10.1109/JPHOT.2019.2916106

Manuscript received March 11, 2019; revised May 4, 2019; accepted May 7, 2019. Date of publication May 20, 2019; date of current version May 31, 2019. This work was supported in part by the National Natural Science Foundation of China under Grant 11674243 and Grant 11674242, in part by the open fund of the air traffic management research institute under Grant KGYJY2018002), and in part by the Fundamental Research Funds for the Central Universities under Grant 3122018D029. Corresponding author: Guizhong Zhang (e-mail: johngzhang@tju.edu.cn).

Abstract: In this paper, we report the results of numerical simulation on vortex-shaped photoelectron momentum spectra of the hydrogen atom irradiated by a pair of time-delayed circularly polarized ultrashort pulses. Spectral alterations including broadening, splitting, and fusion are observed with stronger pulse intensity deploying the quantum wave-packet theory. These alterations of the dynamic interference structure are further investigated to stem from the ac Stark effect, by making the local approximation for an analytical ansatz. In addition, for evaluating the ac Stark effect on the hydrogen atom quantitatively, we propose a nonlinear-curve-fitting algorithm of the ground-state population for extracting the complex Stark coefficient, which we define. We find that the ac Stark effect can be well characterized by the complex coefficient, as supported by the overall agreement between the momentum spectra obtained from the wave-packet theory and the local approximation ansatz. The present research may shed further light on Stark effect in laser atom interactions.

Index Terms: —.

1. Introduction

The Stark effect [1]–[3], discovered by Johannes Stark in 1913, and severing as an important proof for quantum mechanics, is proven to be a mainstay of the undergraduate and graduate physics curricula. For several decades, this prominent process has been investigated in the theoretical and experimental aspects, and remains an interesting theme today [4], [5]. In numerous textbooks, the Stark effect is discussed mostly for a static field or low-frequency pulse [2], [3]. But, if the frequency of a pulse becomes high, and under appropriate conditions, the eigenvalues of an atom will follow only the intensity envelope of the field instead of the instantaneous electric field, which will generate a quasistatic shift of the energy level, which is known as ac Stark effect (or dynamic Stark effect) [5]–[10]. In recent years, with the advent of ultrashort or few-cycle laser pulses, the ac Stark effect has demonstrated some novel features. Chini *et al.* [11] studied the subcycle ac Stark effect of helium atoms ionized with a combined XUV pulses and near-infrared (NIR), and a subcycle energy level shift in helium was found. In 2012, a pioneering work by Demekhin *et al.* [12] discovered that strong interference fringes appear as a new spectral feature in photoelectron spectra of hydrogen

atom ionized with a XUV pulse of carrier frequency 53.6 eV, which far exceeds the hydrogenic ionization potential of 13.6 eV. This interference spectrum was revealed to be caused by the ac Stark effect of hydrogen atom mapped to the continuum via ionization by a single photon of ultrashort laser pulse. Then, similar interference features in the photoionization spectra caused by ac Stark effect were found in molecule [13]. In 2016, Yu *et al.* [5] studied the dynamic process of sequential and non-sequential double ionization in relation to ac Stark effect from joint spectra, illustrating the significance of using photoionization spectra to study the ac Stark effect. However, the ultrashort laser pulses used for photoionization in these methods were only linearly polarized, which seems to be the bottleneck of the investigation of the ac Stark effect using photoionization.

Actually, pertaining to the variants of the exciting laser pulses, a variety of complex pulse combination have been proposed: linearly or circularly polarized [14]–[19], single color or two colors [20]–[23]; and few cycle or many cycles [24]–[28]. Moreover, in 2015, Dijiokap *et al.* [29] designed a combined pulse scheme: two time-delayed weak-to-intermediate-intensity circularly polarized ultrashort laser pulses. By using these combined pulses, they generated a totally new spectral pattern in single ionization of helium atom: vortex-shaped momentum distribution. The induced momentum distributions of the photoionization in the plane of the laser polarization [30] demonstrated a spiral structure or vortex shape [31], [32], which is regarded as the generation of a special Ramsey-type interference of laser-induced electron wave-packet. Numerical simulations showed that the number and shape of the vortex arms in the spiral momentum spectra are sensitive to the time delay and carrier frequency of the combined pulse, which can be applied to investigate the quantum property of atoms or molecules. Moreover, In 2017, Pengel *et al.* [26] verified this kind of vortex-shaped momentum distribution experimentally with pottasium atoms, which opened the way of exploiting time-delayed and circularly polarized laser pulses in investigation of strong field process.

Based upon the sensitivity of the vortex photoionization spectra to the interaction between the combined pulses and atom, we investigate the ac Stark effect on the mechanism and aberration of the vortex-shaped momentum distribution of hydrogen atom ionized with lasers of different carrier frequency and intensity by deploying the quantum wave-packet formalism [33], [34]. It is found that the inner and outer diameters of the vortex-shaped spectra are approximately proportional to the carrier frequency of the combined ultrashort pulses, and the vortex arms appear to split and fuse with increasing the laser intensity. In addition, for evaluating the ac Stark effect on vortex photoionization spectra effectively, we propose a parameter-fitting method to extract the ac Stark coefficient within the wave-packet theory and the local approximation method [35], [36], and careful numerical calculation is performed for studying the real and imaginary parts of the ac Stark coefficient. These novel and interesting observations can serve as an effective and sensitive tool for investigating the ac Stark effect in atoms and molecules.

2. Numerical Methods

The micro-process of hydrogen atom lodged in ultrashort combined laser pulses is the electron ionization from the ac Stark-shifted ground state to the above-ionization-threshold continuum states. The ionization potential of the hydrogen is 13.6 eV, which means that in a weak field a single photon of 13.6 eV or higher can ionize the hydrogen atom preferentially, and generate photoelectron with a kinetic energy of the photon energy minus 13.6 eV. Under strong combined pulses excitation, nevertheless, the photoionization momentum distributions manifest themselves in a complex interference structure instead of a single peak. These photoelectron spectra carry rich information on the atomic energy levels and so on, being beneficial for the investigation of the ac Stark effect.

For a concise and comprehensive description of the ac Stark effect on the photoionization spectra, we use the wave-packet theory and local approximation method to simulate the dynamic process of the photoionization of hydrogen atom by ultrashort combined pulses.

2.1 Quantum Wave-Packet Formalism

In theory, the time-dependent wavefunction is written as a linear combination of the ground state wavefunction and the continuum state ones, ignoring the nonessential states. According to the ref [37], the ac Stark effect arises from the indirectly coupling of the nonessential states (excited bond states) that can not participate in the ionization process. An atom initially in its ground state $|I\rangle$ is ionized into the final continuum state $|\vec{p}\rangle$. Following [38]–[40], we can write the total time-dependent wavefunction of the system as:

$$|\psi(t)\rangle = a_I(t)|I\rangle + \int a_{\vec{p}}(t)|\vec{p}\rangle\, d\vec{p} \tag{1}$$

where a_I and $a_{\vec{p}}$ indicate the time-dependent amplitudes of the initial ground and final continuum states, respectively. The coupled time-dependent equation set for the wavefunctions is obtained by plugging the total wavefunction into the time-dependent Schrodinger equation and projecting onto each eigenstate. According to [12], these coupled equations are written in the following (atomic units are used throughout, or specified if necessary):

$$\begin{cases} i\dot{a}_I(t) = \int a_{\vec{p}}(t)\,\overrightarrow{D_{\vec{p}}}\cdot\overrightarrow{E(t)}d\vec{p} \\ i\dot{a}_{\vec{p}}(t) = \overrightarrow{D_{\vec{p}}}\cdot\overrightarrow{E(t)}a_I(t) + \left(I_p + \frac{\vec{p}^2}{2} - \omega\right)a_{\vec{p}}(t) \end{cases} \tag{2}$$

Here, $\overrightarrow{D_{\vec{p}}} = \langle\vec{p}|z|I\rangle$ expresses the dipole transition matrix element, and I_p is the photoionization potential of the hydrogen atom. The electric field associated with the combined laser pulses, $\overrightarrow{E(t)}$, which is supposed to be polarized in the x-y plane of the Cartesian coordinates in our simulation. Its two components are written as (plus or minus signs determine the left or right helicities):

$$\begin{cases} E_x = \frac{\sqrt{2}}{2}g(t)\cdot E_0\cdot\cos(\omega t) + \frac{\sqrt{2}}{2}g(t+\tau)\cdot E_0\cdot\cos(\omega(t+\tau)) \\ E_y = \frac{\sqrt{2}}{2}g(t)\cdot E_0\cdot\sin(\omega t) - \frac{\sqrt{2}}{2}g(t+\tau)\cdot E_0\cdot\sin(\omega(t+\tau)) \\ g(t) = \exp\left(-\left(\frac{t}{T}\right)^2\right) \end{cases}, \left(-\frac{T}{2} < t < \frac{T}{2}\right) \tag{3}$$

where τ is the time delay between the two polarized ultrashort pulses, T indicates the full width half maximum(FWHM) of the pulse, and E_0 is the peak amplitude of the electric field. For computing the dipole transition matrix element, the initial and final wavefunctions are necessary. We apply the ground-state wavefunction of the real hydrogen atom in three dimensions as the initial state:

$$\varphi_{100} = R_{10}Y_{00} = \pi^{-1/2}\exp(-r) \tag{4}$$

In present calculation, the final wavefunction is expressed as the rigorous eigenfunction for the continuum states of the hydrogen atom:

$$\varphi_{klm} = R_{kl}Y_{lm} \tag{5}$$

R_{klm} can be written as a sophisticated expression:

$$R_{kl} = \frac{1}{(2l+1)!}\frac{2\sqrt{k}}{1-\exp(-2\pi/k)}\cdot\prod_{s=1}^{l}\sqrt{s^2+k^{-2}}(2kr)^l\exp(-ikr)\cdot F(i/k+l+1, 2l+2, 2ikr) \tag{6}$$

Here, $F(i/k+l+1, 2l+2, 2ikr)$ is the confluent hypergeometric function. Alternatively, for a simple expression, the final wavefunctions can also be presented by,

$$\varphi_k^{3D} = (2\pi)\exp(ikz) \tag{7}$$

Here k is the wave vector. When computing the dipole transition matrix element, we normalize both functions given above. Note that in this paper, the sophisticated expression of the final continuum state is used.

2.2 Local Approximation

The method of the quantum wave-packet formalism is an exact technique for the photoionization spectra calculation. Now, we would like to investigate the ac Stark effect by making approximations which can allow us to arrive at concise analytic ansatz, and give a quantitative picture of the ac Stark effect within the quantum wave-packet framework. In the local approximation method, the ground state $|I\rangle$ can be manifested with the signal envelope and simplified parameters, which is beneficial to study the ac Stark effect.

Specifically, equation (2) can be translated into

$$i\dot{a}_I(t) = \left(\Delta - \frac{i}{2}\Gamma\right) g^2(t)\, a_I(t) \tag{8}$$

which can then be solved explicitly as:

$$a_I(t) = \exp\left[(-i\Delta - \Gamma/2)\int_{-\infty}^{t} g^2(t')dt'\right] \tag{9}$$

Here, we define a novel parameter, referred to as the ac Stark coefficient, as:

$$S = -i\Delta - \frac{\Gamma}{2} \tag{10}$$

Where Δ can describe the shift of the energy level of the ground state $|I\rangle$ immersed into the dressed continua, and Γ can elucidate the loss of the population of the ground state $|I\rangle$ due to photoionization into the final continua. This newly defined parameter can explicitly and comprehensively characterize the ac Stark effect acting on the photoionization momentum spectra generated by the ultrashort combined pulses.

According to [38], [41], we have:

$$\begin{aligned} a_{\vec{p}}(t) = & -i\left\{\frac{1}{2}\overrightarrow{D_{\vec{p}}}\overrightarrow{E(t)}\right\}\exp\left(-i\left(I_p + \frac{\vec{p}^2}{2} - \omega\right)t\right)\int_{-\frac{T}{2}}^{t} g(t') \\ & \times \exp\left(S\cdot\int_{-\frac{T}{2}}^{t'} g^2(t'')dt'' + i\left(I_p + \frac{\vec{p}^2}{2} - \omega\right)t'\right)dt' \end{aligned} \tag{11}$$

The photoionization spectra, $\sigma(\vec{p})$, can be expressed as $\sigma(\vec{p}) = |a_{\vec{p}}(\frac{T}{2})|^2$, so that we can obtain the following explicit approximate expression for the spectra:

$$\sigma(\vec{p}) = \left[\frac{1}{2}\overrightarrow{D_{\vec{p}}}\overrightarrow{E(t)}\right]^2\left|\int_{-\frac{T}{2}}^{\frac{T}{2}} g(t')\exp\left(S\cdot\int_{-\frac{T}{2}}^{t'} g^2(t'')dt'' + i\left(I_p + \frac{\vec{p}^2}{2} - \omega\right)t'\right)dt'\right|^2 \tag{12}$$

In addition, the photoelectron momentum spectra can also be transformed into photoelectron energy spectra.

2.3 Nonlinear Curve-Fitting

So far, we have proposed the quantum wave-packet formalism for simulating the photoionization momentum spectra, and further developed a simple local approximation method for reproducing distinct photoionization momentum spectra. Now, we would design a method for evaluating the ac Stark effect of the ground state acting on the photoelectron momentum spectra. It should be able to extract the complex Stark coefficient that we defined before, it is the multi-parameter nonlinear curve-fitting scheme from both the wave-packet theory and local approximation.

By defining the time-dependent amplitude of the population of ground state under the quantum wave-packet formalism as $\alpha_I'(t)$ and using Eq. (11), we can construct the following equation by the

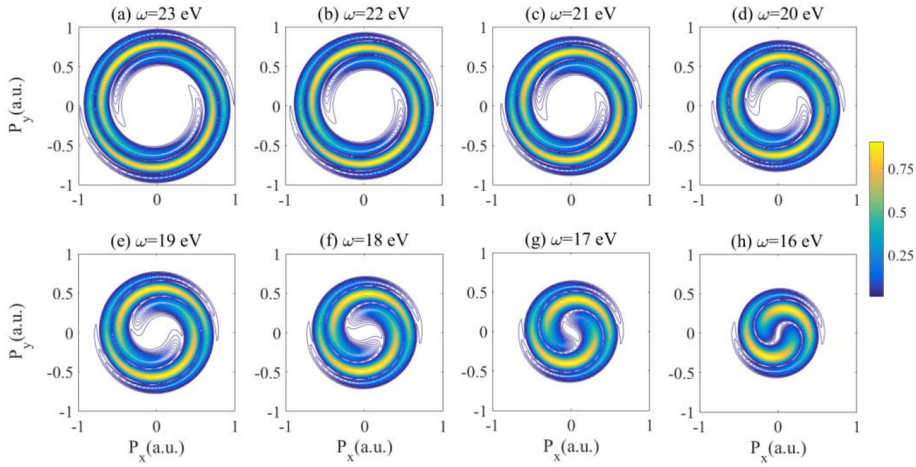

Fig. 1. Carrier frequency dependence of the vortex-shaped photoionization spectra of hydrogen atom exposed to a pair of time-delayed circularly polarized ultrashort pulses: carrier frequency: $\omega = 23$, 22, 21, 20, 19, 18, 17, 16 eV, laser intensity $I = 10^{15}$ W/cm^2, the pulse FWHM $T = 2$ o.c., time delay $\tau = 3$ o.c. The simulation method is based on the exact wave-packet theory.

nonlinear least squares method:

$$G = \sum_{t=t_1}^{t_n} \left| \left(a'_I(t) - \exp\left[\left(-i\Delta - \frac{\Gamma}{2} \right) \int_{-\infty}^{t} g^2(t') dt' \right] \right) \right|^2, \left(-\frac{T}{2} \le t_1, t_2, \ldots, t_n \le \frac{T}{2} \right) \quad (13)$$

Because the energy level shift Δ and population loss Γ are all constants for the ground state for fixed laser parameters, the quantity of $S = -i\Delta - \Gamma/2$ must be a constant. When G is minimum, the corresponding value of the as Stark coefficient S will be the solution, the extracted Stark coefficient will then be used to evaluate the extent of the ac Stark effect in relation to the vortex spectral alterations. Our extensive numerical simulation has been implemented with both matrix algorithm and the fourth-order Runge-Kutta algorithm. The simulated results have been checked for convergence and consistency by using finer time, momentum and energy grids.

3. Simulation Results and Discussion

Radiating the hydrogen atom with a pair of polarized ultrashort pulses with different carrier frequencies, we study structural variation of the vortex-shaped photoionization spectra by the method of quantum wave-packet formalism, and plot a series of these spectra in Fig. 1. It is seen that with the increase of the carrier frequency from 16 eV to 23 eV, the inside and outside diameters of the vortex patterns enlarge gradually, and the vortex arms lengthen from two circles to three circles. These phenomena manifest that the vortex-shaped interference streaks induced by polarized combined pulses have a relationship with the carrier frequency of the pulse combination. In fact, the energy of the pulses overcomes the ionization potential of the hydrogen atom, and the excess energy transfers to the kinetic energy of the ionized electron. Therefore, higher carrier-frequency pulses will induce vortex-shaped momentum pattern with greater momentum values, i.e., bigger vortex radii as shown in Fig. 1. In the traditional ac Stark effect, because the carrier-frequency is too high, the energy level shift just follows in time the square of the envelope of the electric field of the pulse, having no relation with the carrier frequency. However, in Fig. 1, the energy lever shift is associated with the carrier frequency of the pulse combination, which is different from the performance of traditional ac Stark effect. In our view, this phenomena is mainly due to the interplay between two time delayed pulses. In Fig. 2, we further demonstrate that the sectional views of the vortex-shape photoionization spectra vary with the carrier frequency, as plotted along the direction of P_x ($P_y = 0$). In addition to the observations described above, it can also be seen that when the carrier

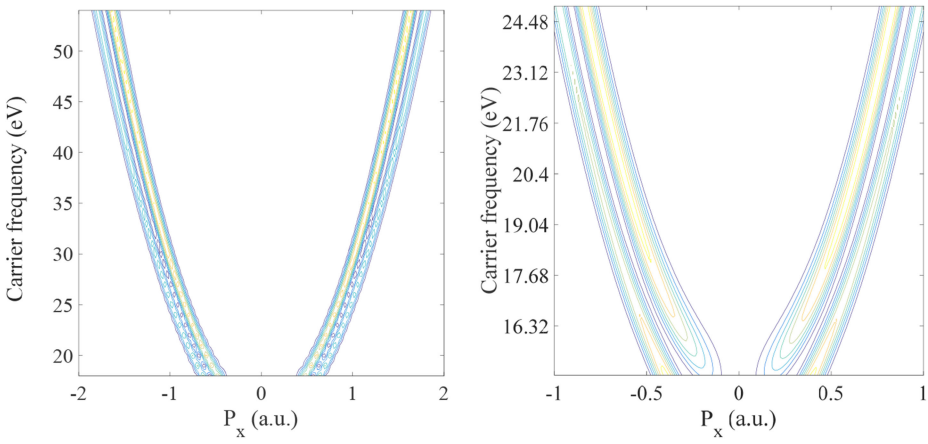

Fig. 2. The sectional view of the vortex-shaped photoionization spectra of hydrogen atom ionized by two time-delayed circularly polarized ultrashort pulses with different carrier frequencies along the P_x-direction ($P_y = 0$). The parameters of the combined pulses is set to be: laser intensity $I = 10^{15}$ W/cm^2, pulse FWHM $T = 2$ o.c., time delay $\tau = 3$ o.c. The right pattern is the partial enlargement of the left one. The simulation method is based on the exact wave-packet theory.

frequency is higher than 25 eV, the diameter of the vortex pattern is linearly proportional to the carrier frequency, and the width of the vortex arms is nearly constant. This feature can be used to measure the high carrier frequency of the pulse combination in some sense. If the carrier frequency is below 25 eV, the vortex arms are broadened slightly with the decrease of the carrier frequency, and the diameter of the vortex pattern shows a nonlinear relationship with the carrier frequency. It is worthy of noting that we reach similar observations for other laser pulse combinations which generate left circularly polarized vortices.

As is well known, an important outcome of the ac Stark effect is the aberration of the photoionization spectra with the increase of the laser pulse intensity. Thus, for exploring the relationship between the intensity of the combined laser pulses and the Stark effect reflected in the vortex spectra, we simulate and plot eight vortex-shaped patterns corresponding to laser intensities of 10^{15}, 1.1×10^{16}, 2.1×10^{16}, 3.1×10^{16}, 4.1×10^{16}, 5.1×10^{16}, 6.1×10^{16}, and 7.1×10^{16} W/cm^2 in Fig. 3. From the eight vortex spectra, we readily observe the following interesting phenomena: (1) the total widths of the vortex arms expand with the increase of the intensity of ultrashort combined pulses, which results in the shrink of the inner diagram of the vortex spectra. Specifically, the inner areas of the vortex patterns nearly disappear at high intensities, as shown by the vortex spectra of Fig. 3(e), (f), (g), and (h); (2) as shown in Fig. 3(a), (b), and (c), the spectral intensities between the two neighboring vortex arms are boosted with increasing pulse intensity. Ultimately, in Fig. 3(c), the vortex-shaped pattern appears to fuse into an annular spectrum; (3) In Fig. 3(e), (f), (g), and (h), when the intensity of combined laser pulse continues to increase, the fused annular photoionization spectra start to show some new structures involving two thick vortex arms in the inner ring and two thin ones in the outer ring. The four vortex arms are weaker than the ones generated by the laser pulses of lower intensities in Fig. 3(a) and (b). The above three observations involve broadening, splitting, and fusion of the vortex spectra. With the following simulations of the comparison between exact and approximate methods, we can conclude that they are all induced by the ac Stark effect. Usually, the ac Stark effect will manifest spectral splitting in intense laser field, the above results by our proposed pulse combination demonstrate the splitting and fusion of the vortex-shaped spectra, which are new physical phenomena. In the following, we decipher our observations in terms of the ac Stark effect under the local approximation which analytically explains the dynamic alterations of the momentum spectra. Namely, the vortex-shaped photoionization spectra are found to gradually evolve from the simple two-arm structure into the complicated structure with inner and outer arms. For clarity, we also give the sectional view of the vortex spectra with different laser intensities along the P_x axis in Fig. 4, where we can observe the broadening, splitting and fusion of the spectral

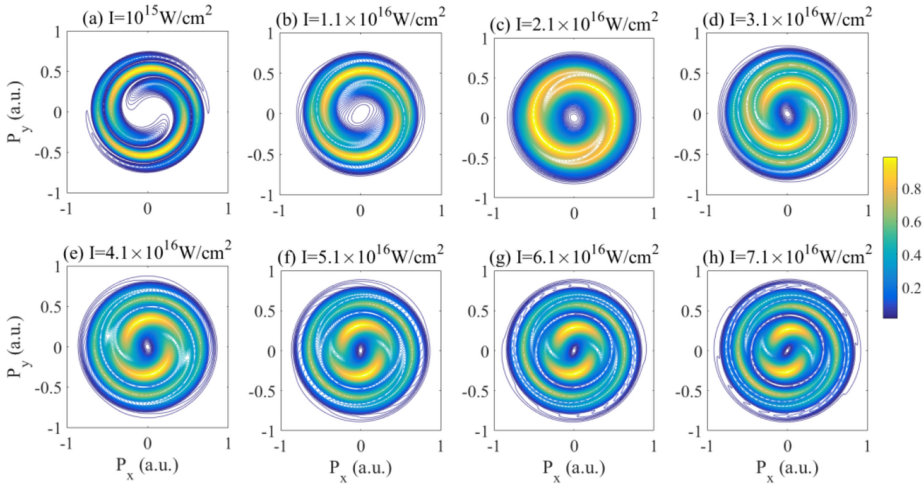

Fig. 3. Intensity dependence of the vortex-shaped photoionization spectra of hydrogen atom exposed to a pair of time-delayed circularly polarized ultrashort pulses: carrier frequency: $\omega = 17.6$ eV, laser intensity I $= 10^{15}$, 1.1 $\times$ 10^{16}, 2.1 $\times$ 10^{16}, 3.1 $\times$ 10^{16}, 4.1 $\times$ 10^{16}, 5.1 $\times$ 10^{16}, 6.1 $\times$ 10^{16}, 7.1 $\times$ 10^{16} W/cm^2, the pulse FWHM T $= 2$ o.c., time delay $\tau = 3$ o.c. The simulation method is based on the exact wave-packet theory.

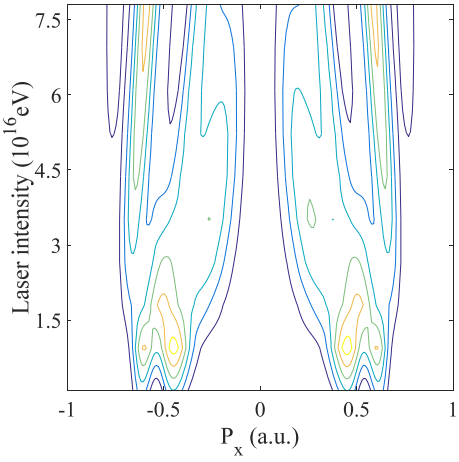

Fig. 4. The sectional view of the vortex-shaped photoionization spectra of hydrogen atom ionized by two time-delayed circularly polarized ultrashort pulses with different laser intensities along the Px-direction ($P_y = 0$). The parameters of the combined pulses are set to be: carrier frequency $\omega = 17.6$ eV, pulse FWHM T $= 2$ o.c., time delay $\tau = 3$ o.c. The simulation method is based on the exact wave-packet theory.

feature more clearly. Our studies show that the ac Stark shift is negative in the intensity range of 3.1 $\times$ 10^{16} W/cm^2 to 7.1 $\times$ 10^{16} W/cm^2, which is normal for the ac Stark effect, but in the intensity range of 1.1 $\times$ 10^{15} W/cm^2 to 3.1 $\times$ 10^{16} W/cm^2, the ac Stark shift is positive, which is an abnormal phenomenon. In our view, these abnormal structures in the photoelectron spectra originate from the strong dynamic interference of the photoelectrons of the same kinetic energy emitted at different times, which is similar to the strong interference fringes discovery by Demekhin *et al.* [12] in 2012.

From the time-dependent population of the ground state of the hydrogen atom calculated with the wave-packet theory and deploying Eq. (9), we can fit the time-varying population curves to get the values of the parameters S (Δ and Γ) of the ac Stark effect, as shown by the middle row in Fig. 5. Specifically, according to Eq. (13), the values of Δ and Γ that is given in Fig. 5 can make G minimum. We plot the vortex-shaped photoelectron spectra obtained with the exact wave-packet

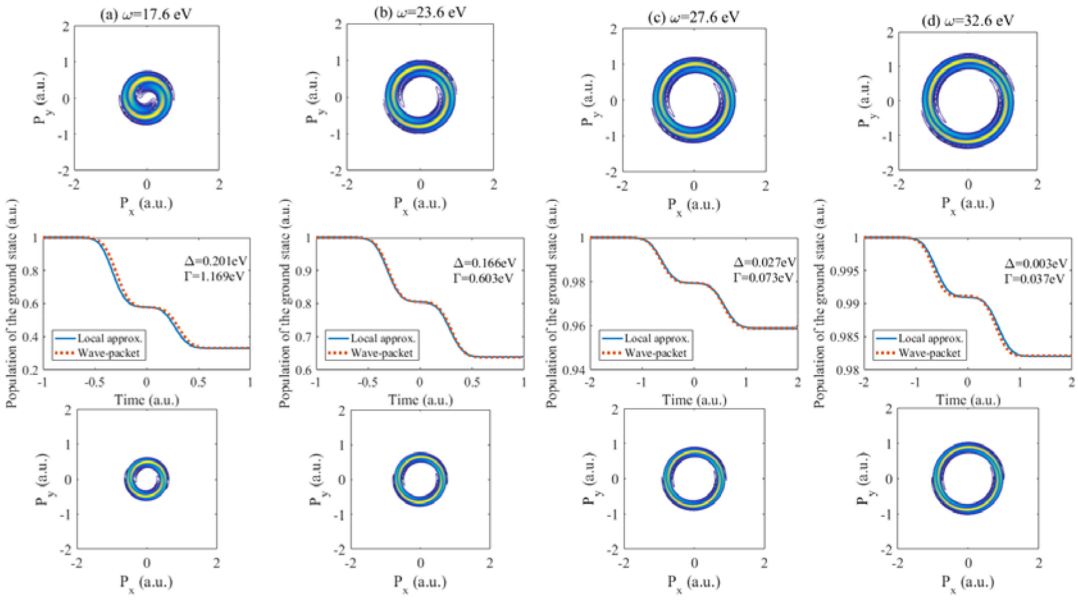

Fig. 5. Comparison of the vortex spectra of hydrogen atom exposed to combined pulses of pulse FWHM T = 2 o.c., intensity I = 5 × 10^{15} W/cm^2, and time delay τ = 3 o.c. Top row: photoelectron spectra for pulse FWHM T = 2 o.c., intensity I = 5 × 10^{15} W/cm^2, and time delay τ = 3 o.c., computed exactly by the wave-packet theory with the parameters of ω = 17.6, 23.6, 27.6, 32.6 eV (from left to right). Bottom row: vortex spectra calculated under the local approximation for the same carrier frequencies with the corresponding Stark coefficients: Γ = 1.169, 0.603, 0.073, 0.037 eV and Δ = 0.201, 0.166, 0.027, 0.003 eV (from left to right). Middle row: time variation of the population of the ground state of the hydrogen atom exposed to combined pulses with the same carrier frequencies. The dotted curves are computed exactly with the wave-packet theory, compared with the solid curves that are best fitted under the local approximation. The extracted Stark coefficients are used for plotting the vortex spectra in the bottom row.

theory (top row), and the local approximation method (bottom row) using the fitted Stark coefficient S = $-\Delta$i$-\Gamma$ in Eq. (12) in the same figure.

Compared to the photoelectron vortex spectra simulated with the exact wave-packet theory (top row in Fig. 5), the characteristics of the vortex spectra generated by the local approximation method exhibit the following properties: (1) the photoelectron momentum distributions still show vortex shapes, and are fairly similar to the ones calculated by the wave-packet theory, in respect of the positions of vortex arms; (2) the outer diameters of the vortex arms simulated by the two approaches both expand with the increase of the carrier frequency, which is also in agreement with the simulations presented in Fig. 2; (3) the vortex arms by the local approximation are wider than the ones by the wave-packet method. These overall agreements between the vortex pattern alterations obtained via the two methods prove that the local approximation method can semi-quantitatively describe the photoionization vortex spectra pertaining to ac Stark effect. On the whole, these comparisons also demonstrate that the as Stark coefficients obtained by the nonlinear curve-fitting can describe approximately the photoionization spectra of the hydrogen atom.

Pertaining to the ac Stark effect as shown in the middle row of Fig. 5, one sees that the population of the ground state descends with time, and in two steps. This two-stage curve structure originates from the two time-delayed pulses, which reflects the fact that the first pulse ionizes the hydrogen atom resulting in the first population loss or the first stage in the curves in the middle row of Fig. 5, and the second or time-delayed pulse further ionizes the atom resulting in a secondary population decrease or the second stage. One can see clearly from Fig. 5 (middle row) that for the four carrier frequencies used in the simulation, the fitted curves by local approximation method agree pretty well with the ones calculated with the exact wave-packet method, which justifies that Eq. (9) can effectively elucidate the ac Stark coefficient S = $-\Delta$i$-\Gamma$/2 in the local approximation

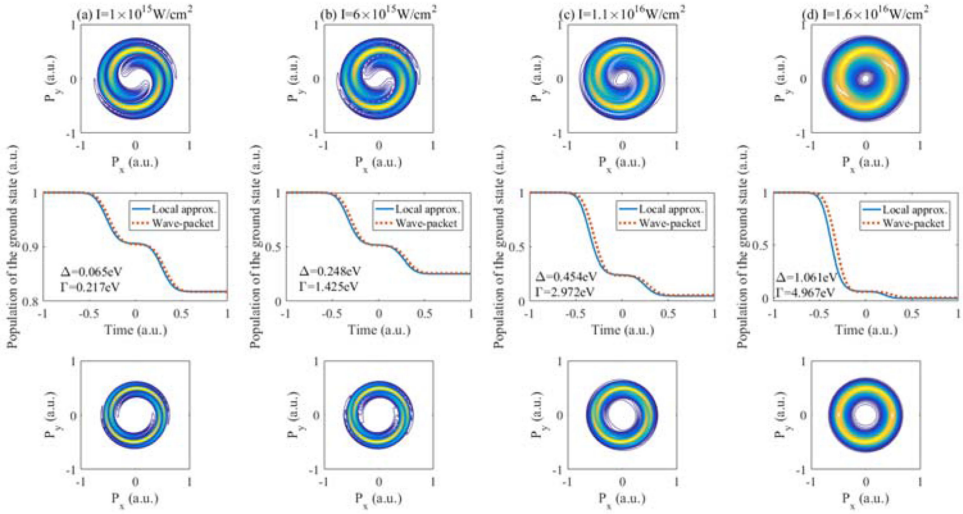

Fig. 6. Comparison of the photoelectron vortex spectra of hydrogen atom exposed to combined pulses. Top row: vortex spectra for pulse FWHM T = 2 o.c., carrier frequency $\omega = 17.6$ eV, and time delay $\tau =$ 3 o.c., computed exactly by the wave-packet theory with increasing intensities I = 1×10^{15}, 6×10^{15}, 1.1×10^{16}, 1.6×10^{16} W/cm^2 (from left to right). Bottom row: vortex spectra calculated under the local approximation for the same intensities, with $\Gamma = 0.065$, 0.248, 0.454, 1.061 eV and $\Delta = 0.217$, 1.425, 2.972, 4.967 eV (from left to right). Middle row: time variation of the population of the ground state of the hydrogen atom. The dotted curves are computed exactly with the wave-packet theory, compared with the solid curves that are best fitted under the local approximation. As in Fig. 5, the extracted Stark coefficients are used for plotting the vortex spectra in the bottom row.

method. Through our curve fitting in Fig. 5, the corresponding parameters of the ac Stark effect are obtained as $\Gamma = 1.169$, 0.603, 0.073, 0.037 eV and $\Delta = 0.201$, 0.166, 0.027, 0.003 eV, for $\omega = 17.6$, 22.6, 27.6, 32.6 eV, respectively. We find that the real part/imaginary part/module of the coefficient coefficient decreases with the increase of the carrier frequency. This phenomenon can be revealed and explained by the mathematical expression of the Stark coefficient [12]: the carrier frequency appears in the denominator of the formula so that the ac Stark coefficient decreases with increasing carrier frequency.

In order to further verify the ac Stark nature resulting in the alterations of the vortex momentum spectra, we also implement the simulation of the spectra generated with varying laser intensities. We present these vortex-shaped photoelectron spectra by the exact wave-packet theory (top row), and the local approximation method (bottom row) in Fig. 6. The intensity range used in this simulation is between 1×10^{15} and 1.6×10^{16} W/cm^2. Besides the characteristics of the photoionization spectra observed from Fig. 5, we also observe that the fusion of vortex arms is exactly reproduced using the local approximation method, as the laser intensity is increased. This performance corroborates that the ac Stark effect indeed induces the observed spectral pattern alterations, in addition to the justice of the nonlinear curve-fitting of the ground state population in characterizing the photoionization spectra effectively.

With respect to the ac Stark effect with increasing pulse intensities, we also plot, in the middle row of Fig. 6, the temporal variation of the population of the ground state. One sees clearly that the population depletion gradually changes from a two-step nature to an almost one-step feature, as the laser intensity is enhanced. This phenomenon is readily explained: as the laser intensity increases nearly all the electrons in the ground state are ionized by the first pulse so that the population loss due to the second pulse becomes negligible (see similar discussion before). By using the complex Stark coefficient $S = -\Delta i - \Gamma/2$ and our nonlinear curve-fitting method again, we are able to extract the parameters of the ac Stark effect to be: $\Gamma = 0.065$, 0.248, 0.454, 1.061 eV and $\Delta = 0.217$, 1.425, 2.972, 4.967 eV, corresponding to laser intensities of I = 1×10^{15}, 6×10^{15}, 1.1×10^{16}, $1.6 \times$

10^{16} W/cm^2. These data show that the ac Stark coefficient increases approximately proportionally with the laser intensity, which is in line with the previous experiments of the Stark effect [2].

The overall agreement between the momentum spectra simulated using the exact wave-packet theory and the local approximation method, as illustrated in Fig. 5 and Fig. 6, proves that the ac Stark effect induces the spectral alterations as the carrier frequency and laser intensity are varied, considering the approximations made in the local approximation method. However, detailed comparison between these spectra indeed shows some disparity between the vortex patterns obtained with these two approaches. The deviation can be understood if one examines the conditions in deriving the local approximation. The ac Stark effect mandates that there be many carrier cycles [4], [12], [42] under the envelope and the carrier frequency be high enough. The local approximation treatment also requires that the carrier frequency be high [12], [35], [43]. In our situation, we use pulse combination with pulse FWHMs of two optical cycles (Fig. 5 and Fig. 6) because the vortex-shaped momenta will be generated only with wide enough bandwidth or short pulse FWHM, as discussed in [26]. Therefore, the deviation can be explained. The trends of vortex alterations and the essential physics captured by the local approximation approach support the origin of the dynamic ac Stark effect imprinted in the vortex momentum spectra.

4. Conclusion

For exploring the effect of the ac Stark effect in the photoionization process elucidated by the vortex-shaped momentum spectra, we design a laser field involving two time-delayed circularly polarized ultrashort pulses and use them to ionize the hydrogen atom. Deploying the method of the exact wave-packet theory, we successfully produce the vortex-shaped momentum distributions through numerical simulation, and investigate the ac-Stark-induced spectral alterations by varying the carrier frequency and laser intensity, and making the local approximation. The fairly good reproduction of the alterations of the vortex momentum spectra by the local approximation method reveals the ac Stark origin of these alterations. Compared with the other methods of ac Stark description, the

In addition, we are able to extract the complex Stark coefficient from the time-varying population of the ground state by the nonlinear curve-fitting algorithm. Compared with other methods of ac Stark description based upon complex linear streak in the spectra, our approach can extract more characteristic information from the regular vortex arms, thereby manifesting more features of the ac Stark effect. We anticipate that the dynamic evolvement of the vortex-shaped momentum spectra in relation to the Stark effect could shed light on deeper investigation on strong field processes in atoms and molecules. For the subsequent research, we can select the Helium or other inert atoms as the excited atom for investigating the ac Stark effect.

References

[1] S. H. Autler and C. H. Townes, "Stark effect in rapidly varying fields," *Phys. Rev.*, vol. 100, pp. 703–722, 1955.
[2] E. Merzbacher, *Quantum Mechanics*, 3rd ed. New York, NY, USA: Wiley, 1998, p. 3.
[3] H. C. Ohanian, *Principles of Quantum Mechanics*. Engle wood Cliffs, NJ, USA: Prentice-Hall, 1990.
[4] N. B. Delone and V. P. Krainov, "AC Stark shift of atomic energy levels," *Phys. Uspekhi*, vol. 42, pp. 669–687, 1999.
[5] C. Yu and L. B. Madsen, "Sequential and nonsequential double ionization of helium by intense XUV laser pulses: Revealing ac Stark shifts from joint energy spectra," *Phys. Rev. A*, vol. 94, no. 5, 2016, Art. no. 053424.
[6] M. V. Fedorov, *Atomic and Free Electrons in a Strong Light Field*. Singapore: World Scientific, 1997.
[7] L. Allen and J. H. Eberly, *Optical Resonance and Two Level Atoms*. Minneola, NY, USA: Dover: 1987.
[8] C. Gerry and P. Knight. *Introductory Quantum Optics*. Cambridge, U.K.: Cambridge Univ. Press, 2004.
[9] R. Loudon, *The Quantum Theory of Light*. London, U.K: Oxford Univ. Press, 2000.
[10] W. L. Zhang, X. M. Wu, F. Wang, R. Ma, X. F. Li, and Y. J. Rao, "Stark effect induced microcavity polariton Solitons," *Opt. Exp.*, vol. 23, no. 12, pp. 15762–15767, 2015.
[11] M. Chini, B. Zhao, H. Wang, Y. Cheng, S. X. Hu, and Z. Chang, "Subcycle ac stark shift of helium excited states probed with isolated attosecond pulses," *Phys. Rev. Lett.*, vol. 109, 2012, Art. no. 073601.
[12] P. V. Demekhin and L. S. Cederbaum, "Dynamic interference of photoelectrons produced by high-frequency laser pulses," *Phys. Rev. Lett.*, vol. 108, no. 25, 2012, Art. no. 253001.
[13] C. Yu, N. Fu, T. Hu, G. Zhang, and J. Yao, "Dynamic stark effect and interference photoelectron spectra of H_2+," *Phys. Rev. A*, vol. 88, no. 5, 2013, Art. no. 043408.

[14] L. Peng, E. A. Pronin, and A. F. Starace, "Attosecond pulse carrier-envelope phase effectson ionized electron momentum and energy distributions: Roles of frequency, intensity and an additional IR pulse," *New J. Phys*, vol. 10, no. 2, 2008, Art. no. 025030.
[15] P. L. He, C. Ruiz, and F. He, "Carrier-envelope-phase characterization for an isolated attosecond pulse by angular streaking," *Phys. Rev. Lett.*, vol. 116, no. 20, 2016, Art. no. 203601.
[16] M. Klaiber, E. Yakaboylu, and K. Z. Hatsagortsyan, "Above-threshold ionization with highly charged ions in superstrong laser fields. I. Coulomb-corrected strong-field approximation," *Phys. Rev. A*, vol. 87, no. 2, 2013, Art. no. 023417.
[17] C. Figueira de Morisson Faria, H. Schomerus, X. Liu, and W. Becker, "Electron-electron dynamics in laserinduced nonsequential double ionization," *Phys. Rev. A*, vol. 69, no. 4, 2004, Art. no. 043405.
[18] M. Abu-samha and L. B. Madsen, "Interrogation of orbital structure by elliptically polarized intense femtosecond laser pulses," *Phys. Rev. A*, vol. 84, no. 2, 2011, Art. no. 023411.
[19] X. S. Zhu, Q. B. Zhang, W. Y. Hong, P. X. Lu, and Z. Z. Xu, "Laser-polarization-dependent photoelectron angular distributions from polar molecules," *Opt. Exp.*, vol. 19, no. 24, pp. 24198–24209, 2011.
[20] M. H. Xu *et al.*, "Attosecond streaking in the low-energy region as a probe of rescattering," *Phys. Rev. Lett.*, vol. 107, no. 18, 2011, Art. no. 183001.
[21] J. W. Geng, W. H. Xiong, X. R. Xiao, L. Y. Peng, and Q. Gong, "Nonadiabatic electron dynamics in orthogonal two-color laser fields with comparable intensities," *Phys. Rev. Lett.*, vol. 115, no. 19, 2015, Art. no. 193001.
[22] M. Li *et al.*, "Spatial-temporal control of interferences of multiple tunneling photoelectron wave packets," *Phys. Rev. A*, vol. 92, no. 1, 2015, Art. no. 013416.
[23] Y. Zhou, C. Huang, A. Tong, Q. Liao, and P. Lu, "Correlated electron dynamics in nonsequential double ionization by orthogonal two-color laser pulses," *Opt. Exp.*, vol. 19, no. 3, pp. 2301–2308, 2011.
[24] J. M. Ngoko Djiokap, A. V. Meremianin, N. L. Manakov, S. X. Hu, L. B. Madsen, and A. F. Starace, "Multistart spiral electron vortices in ionization by circularly polarized UV pulses," *Phys. Rev. A*, vol. 94, no. 1, 2016, Art. no. 013408.
[25] M. Harris, C. A. Hill, and J. M. Vaughan, "Optical helices and spiral interference fringes," *Opt. Commun*, vol. 106, no. 4-6, pp. 161–166, 1994.
[26] D. Pengel, S. Kerbstadt, D. Johannmeyer, L. Englert, T. Bayer, and M. Wollenhaupt, "Electron vortices in femtosecond multiphoton ionization," *Phys. Rev. Lett.*, vol. 118, no. 5, 2017, Art. no. 053003.
[27] J. Tan *et al.*, "Determination of the ionization time using attosecond photoelectron interferometry," *Phys. Rev. Lett.*, vol. 121, 2018, Art. no. 253203.
[28] J. Tan *et al.*, "Time-resolving tunneling ionization via strong-field photoelectron holography," *Phys. Rev. A*, vol. 99, 2019, Art. no. 033402.
[29] J. M. Ngoko Djiokap, S. X. Hu, L. B. Madsen, N. L. Manakov, A. V. Meremianin, and A. F. Starace, "Electron vortices in photoionization by circularly polarized attosecond pulses," *Phys. Rev. Lett.*, vol. 115, no. 11, 2015, Art. no. 113004.
[30] E. Hasović, W. Becker, and D. B. Milošević, "Electron rescattering in a bicircular laser field," *Opt. Exp.*, vol. 24, no. 6, pp. 6413–6424, 2016.
[31] K. Yuan, S. Chelkowski, and A. D. Bandrauk, "Photoelectron momentum distributions of molecules in bichromatic circularly polarized attosecond UV laser fields," *Phys. Rev. A*, vol. 93, no. 5, 2016, Art. no. 053425.
[32] M. Li, G. Zhang, X. Ding, and J. Yao, "Symmetric electron vortices of hydrogen ionized by orthogonal elliptical fields," *IEEE Photon. J*, vol. 10, no. 4, Aug. 2018, Art. no. 3300109.
[33] B. M. Garraway and K. A. Suominen, "Wave-packet dynamics: New physics and chemistry in femto-time," *Rep. Prog. Phys.*, vol. 58, pp. 365–419, 1995.
[34] C. Yu and L. B. Madsen, "Core-resonant ionization of helium by intense XUV pulses: Analytical and numerical studies on channel-resolved spectral features," *Phys. Rev. A*, vol. 98, 2018, Art. no. 033404.
[35] L. S. Cederbaum and W. Domcke, "Local against non-local complex potential in resonant electron-molecule scattering," *J. Phys. B*, vol. 14, pp. 4665–4690, 1981.
[36] W. Domcke, "Theory of resonance and threshold effects in electron-molecule collisions: The projection-operator approach," *Phys. Rep.*, vol. 208, pp. 97–188, 1991.
[37] B. J. Sussman, "Five ways to the nonresonant dynamic Stark effect," *Am. J. Phys.*, vol. 79, pp. 477–484, 2011.
[38] E. Pahl, H.-D. Meyer, and L. S. Cederbaum, "Competition between excitation and electronic decay of short-lived molecular states," *Zeitschrift für Physik D Atoms, Molecules Clusters*, vol. 38, pp. 215–232, 1996.
[39] Y.-C. Chiang, P. V. Demekhin, A. I. Kuleff, S. Scheit, and L. S. Cederbaum, "Linewidth and lifetime of atomic levels and the time evolution of spectra and coincidence spectra," *Phys. Rev. A*, vol. 81, 2010, Art. no. 032511.
[40] P. V. Demekhin, S. D. Stoychev, A. I. Kuleff, and L. S. Cederbaum, "Exploring interatomic coulombic decay by free electron lasers," *Phys. Rev. Lett.*, vol. 107, 2011, Art. no. 273002.
[41] P. V. Demekhin and L. S. Cederbaum, "Strong interference effects in the resonant Auger decay of atoms induced by intense x-ray fields," *Phys. Rev. A*, vol. 83, 2011, Art. no. 023422.
[42] P. V. Demekhin, D. Hochstuhl, and L. S. Cederbaum, "Photoionization of hydrogen atoms by coherent intense high-frequency short laser pulses: Direct propagation of electron wave packets on large spatial grids," *Phys. Rev. A*, vol. 88, 2013, Art. no. 023422.
[43] P. V. Demekhin and L. S. Cederbaum, "AC Stark effect in the electronic continuum and its impact on the photoionization of atoms by coherent intense short high-frequency laser pulses," *Phys. Rev. A*, vol. 88, 2013, Art. no. 043414.